Article

Thermal Analysis of a Modular Permanent Magnet Machine under Open-Circuit Fault with Asymmetric Temperature Distribution

Yunfei Liu, Bingyi Zhang *, Ming Zong and Guihong Feng

School of Electrical Engineering, Shenyang University of Technology, Shenyang 110870, China
* Correspondence: zhangby@sut.edu.cn; Tel.: +86-18624016393

Abstract: A modular permanent magnet machine is composed of several stator modules, and the three-phase winding of each module can be controlled independently. The novel modular permanent magnet machine has good abilities in terms of fault tolerance when the machine is exposed to fault conditions. The current of each phase is different and will result in uneven loss distribution in each phase. Heat transfer occurs in the circumferential direction and temperature distribution will be asymmetric in the circumferential direction. This paper proposes a 3D finite element thermal model to accurately calculate the rise in temperature under open-circuit conditions for modular permanent magnet machines. When two modules are in operation, the machine can output rated torque. When one module is in operation and the temperature is 150 °C, the output torque is 0.76 times the rated torque. The temperature of the machine under the one-phase open-circuit condition with a zero-temperature-difference control strategy will be 0.8 °C lower than that with a minimum copper loss control strategy. Finally, a prototype with three stator modules is manufactured and the calculation results are validated by experimental test. It holds great significance for the accurate calculation of a machine with asymmetric temperature distribution in the circumferential direction.

Keywords: modular permanent magnet motor; open circuit; fault tolerant; asymmetric temperature distribution; thermal analysis

1. Introduction

Permanent magnet machines are widely used in various application fields thanks to their high efficiency and torque density. In some special applications, the requirement of reliability and the fault tolerance of machines are much greater, such as in railway traction drive, ship electric propulsion, electric vehicles, and electric aircraft [1–3].

In order to improve the fault tolerance under fault conditions, multi-phase permanent magnet machines are widely used [4,5]. Multi-phase permanent magnet machines need to be controlled by a multi-phase inverter [6]. The fault-tolerance strategy algorithm of a multi-phase machine is complex [7,8]. This paper proposes a novel modular permanent magnet machine, which consists of several stator modules [9,10]. Each stator module has its own three-phase windings that can be controlled independently by its own three-phase inverter. When one stator module or one phase is exposed to fault conditions, the other phases can operate normally. To ensure the output torque remains unchanged, the current in the healthy phase windings should be increased. This will cause a higher temperature in healthy windings. Owing to the limitation of insulation maximum temperature, it is very important to accurately predict the temperature distribution of modular permanent magnet machines under fault-tolerance conditions.

Thermal analysis is important for machine design. In [11], a 3D thermal network model is established to calculate the temperature of a flux-switching permanent magnet double-rotor machine. In [12], a generalized mesh-based thermal network is proposed to obtain temperature distributions instead of the average temperature. The innovation of

the model is to dynamically couple the winding temperature distributions with thermal network meshes in stator. In [13], an electromagnetic–thermal bi-directional coupling method is proposed for thermal analysis of high-speed PMSM considering the assembling gaps. In [14], the temperature of modular-spoke-type permanent magnet machines is calculated, but temperature distributions of the machine under fault conditions are not analyzed. In [15], the transient temperature of switched-flux permanent magnet machine is studied under both healthy and fault conditions. The work of [16] analyzes the temperature distribution of six-phase PMSM with different fault-tolerance modes. In [17], a novel transient 3D lumped-parameter thermal model of a permanent-magnet-assisted synchronous reluctance machine is established to predict the asymmetric temperature distribution under inter-turn short-circuit fault conditions. There is a gap in the literature in terms of a fault-tolerance control strategy that can minimize the temperature under fault conditions and determine the output torque under fault-tolerance conditions within the allowable maximum temperature of insulation, which is filled by this manuscript.

The purpose and objective of this study is to investigate the maximum temperature of the machine under fault conditions as well as the fault-tolerance control strategy that can reduce the rise in temperature. In order to analyze the temperature distribution of the modular permanent magnet machine under fault conditions with an uneven copper loss distribution, a 3D finite element thermal model of a 30-pole 72-slot modular permanent magnet synchronous machine with three stator modules is established. The temperature of each part of the modular permanent magnet machine under rated conditions is calculated. When different numbers of stator modules are in operation, the distribution of stator copper loss is uneven in the circumferential direction and circumferential heat transfer occurs. Therefore, the temperature distribution of the modular permanent magnet machine under asymmetric conditions is mainly analyzed. The temperature distribution under different fault-tolerance control strategies for the one-phase open-circuit condition is analyzed. In order to minimize the rise in temperature of the machine under fault conditions, the fault-tolerance strategy known as zero-temperature-difference control is proposed. The temperature of the machine under the one-phase open-circuit condition with the zero-temperature-difference control strategy will be 0.8 °C lower than that with the minimum copper loss control strategy. A prototype with three stator modules is manufactured and the results of the finite element thermal model and experimental test are in good agreement. It holds great significance for the accurate calculation of a machine with asymmetric temperature distribution in the circumferential direction.

2. Thermal Analysis Model

2.1. Structure of Modular Stator

The stator of a traditional permanent magnet machine is manufactured as a whole, which means modularization cannot be achieved. In order to realize the mechanical separation of each stator module, the stator of the modular permanent magnet machine is composed of several stator modules, and all of the stator modules are assembled together in the circumferential direction. The structure of the modular stator permanent magnet machine is shown in Figure 1.

The key to the modularization of stator and the independence of each stator module is that the machine adopts the combination of the two unequal span windings. In one stator module, the windings are composed of small span coils and large span coils. The difference from traditional windings is the change in the connection of the end winding. The effective section of the winding in the stator slot is not changed. The diagram of the winding connection is shown in Figure 2.
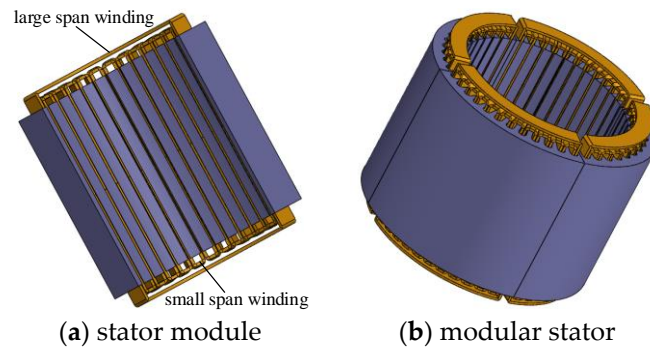
(**a**) stator module   (**b**) modular stator

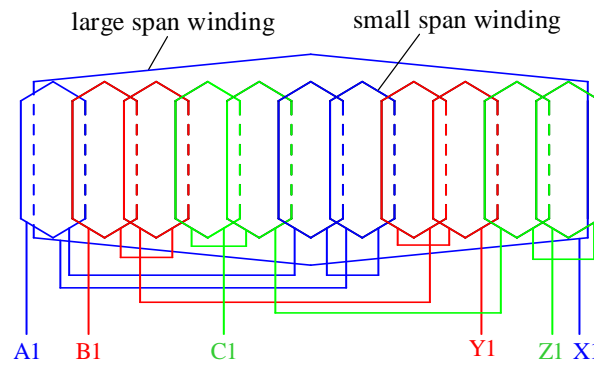**Figure 1.** Structure of stator.

Figure 2. Winding connection of the stator module.

Each module has its own three-phase windings and the windings in each module are not connected to the windings in other stator modules. Each of the three-phase windings are controlled independently by its own inverter. The current in each stator module can be the same, but it can also be different. When one stator module or one inverter fails, it will not influence the other modules, and the other healthy modules can continue to operate. The current in the healthy modules can be adjusted to keep the rated output torque unchanged. Novel modular stator permanent magnet machines have great abilities in terms of fault tolerance.

2.2. Thermal Field Model

The variation in the thermal conductivity of material with the position and temperature of the machine is not considered. In the Cartesian coordinate system, the governing equation of the temperature field is as follows:

$$
\begin{cases}
\frac{\partial}{\partial x}\left(\lambda_x \frac{\partial T}{\partial x}\right) + \frac{\partial}{\partial y}\left(\lambda_y \frac{\partial T}{\partial y}\right) + \frac{\partial}{\partial z}\left(\lambda_z \frac{\partial T}{\partial z}\right) + q_v = 0 \\
-\lambda_n \frac{\partial T}{\partial n} = \alpha(T - T_0)
\end{cases}
\tag{1}
$$

where λ_x, λ_y, λ_z, and λ_n are the thermal conductivity coefficients in the x, y, z, and n directions, respectively. q_v is the heat flux density of each part of the machine, α is the equivalent heat dissipation coefficient, T is the temperature, and T_0 is the temperature of the environment.

In order to facilitate the analysis, some assumptions and equivalence of 3D thermal field model need to be made as follows:

(1) It is assumed that the slots are filled with copper and equivalent insulation. The equivalent model is shown in Figure 3.

(2) The end winding is equivalent to the rod structure, and the resistance of the large-span coil is ignored.

(3) The variation in the thermal conductivity with temperature of all materials used in the machine is ignored.
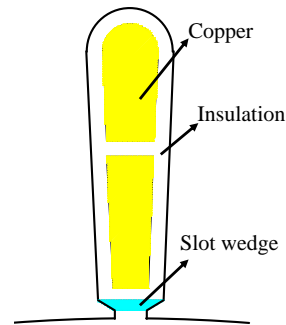
(4) The thermal radiation is not considered.

Figure 3. Schematic of the equivalent winding.

The thermal conductivity of the equivalent insulation material filled in the stator slot can be expressed as follows:

$$\lambda_1 = \sum_{i=1}^{n} h_i \Big/ \left(\sum_{i=1}^{n} h_i / \lambda_i \right) \tag{2}$$

where λ_i is the equivalent heat dissipation coefficient of the material in the stator slot and h_i is the average thickness of the insulation material. The insulation materials in the slot include the following: slot insulation, layer insulation, the paint film insulation of the wire, and the impregnated paint insulation. Here, the thickness of the layer insulation is 0.3 mm and that of the wire wrap is 0.06 mm. The thermal conductivity of all of the materials used in the machine is shown in Table 1.

Table 1. Thermal conductivity of material (W/(m·°C)).

Material	X	Y	Z
Stator core (DW470)	39	39	4.43
Rotor core (DW470)	39	39	4.43
Winding (Copper)	385	385	385
Equivalent insulation	0.27	0.27	0.27
PM (N38UH)	9	9	9
Slot wedge	0.2	0.2	0.2
Shaft (Steel)	45	45	45

The cooling mode of the machine is the natural convention. The equivalent heat dissipation coefficient was obtained from references. It is the same as in the conventional machines, so it is not mentioned. Because the rated speed is 100 r/min, the variation in iron loss and eddy current loss of the permanent magnet with temperature is not considered. In order to accurately calculate the temperature of the machine, the copper loss of the machine must be accurately calculated. The resistance of the windings rises linearly with the increase in temperature during the operation of the machine. Therefore, the factor should be considered in calculating the copper losses:

$$P_{cu} = 3MI^2R \tag{3}$$

$$R = R_0[1 + \theta(T - T_0)] \tag{4}$$

where M is the number of stator modules of the machine. I is the root mean square (rms) current of the one-phase winding in one module. T is the working temperature of the windings and T_0 is the environment temperature. R_0 and R are the resistances of one phase in one module at the initial and steady temperatures, respectively. θ is the temperature coefficient of resistance. The core loss is calculated using FEA methods. The influence of current on iron loss is ignored.

The process of thermal analysis of the modular permanent magnet machine is shown in Figure 4.
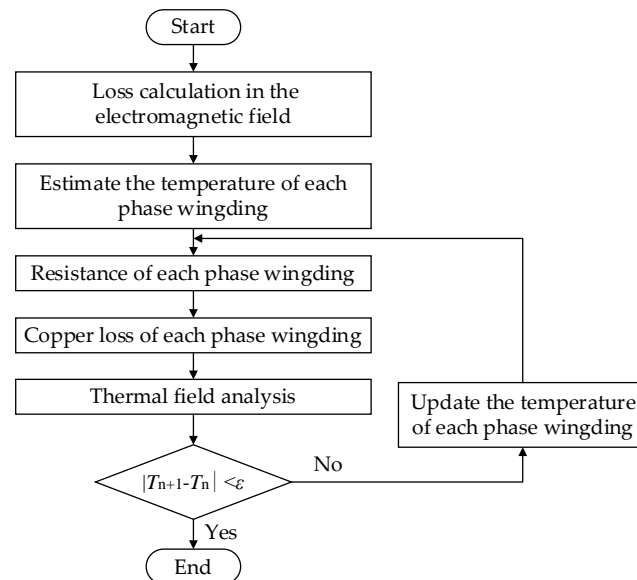

Figure 4. Flow chart of the electromagnetic–thermal coupled method.

3. Thermal Analysis

3.1. Thermal Analysis under the Rated Condition

This paper mainly analyzes the asymmetrical temperature distribution in the circumferential direction of the modular permanent magnet machine, for which the full model of the machine must be built. The main design parameters of the modular permanent magnet machine are shown in Table 2.

Table 2. Parameters of the modular permanent magnet machine.

Parameter	Values and Unit
Rated power	12 kW
Rated voltage	380 V
Frequency	25 Hz
Number of poles	30
Rated current (I_N)	20 A
Rated torque (T_N)	1146 Nm
Number of stator slots	72
Stator external diameter	520 mm
Stator inner diameter	390 mm
Core length	220 mm
Air gap length	0.8 mm
Number of rotor slots	72
No-load back EMF	212 V
Number of modules	3
Small span	2
Large span	22
Efficiency	90.5%
Power factor	0.98

Figure 5 shows the temperature distribution of the modular permanent magnet machine under the rated condition. The cooling condition at the end winding is poor, so the highest temperature occurs at the end winding. The copper loss of the modular permanent magnet machine is uniformly distributed in the circumferential direction under the rated condition, while the temperature distribution of the machine will not be asymmetrical in

the circumferential direction. The maximum temperature is low under the rated condition. The rated temperature is not high in the design process because the machine requires strong fault tolerance. The maximum temperature occurs at the end winding owing to the poor heat dissipation conditions. The length of the large-span coil is short, so the uneven copper loss distribution caused by the increase in resistance can be ignored.
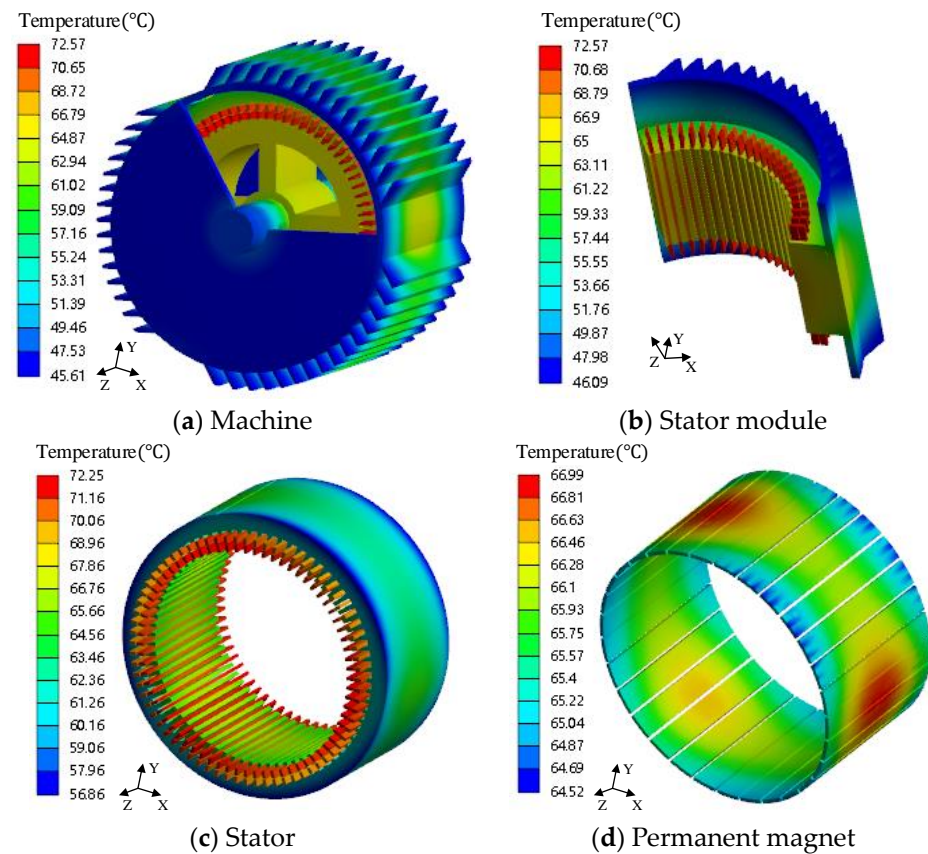

(**a**) Machine

(**b**) Stator module

(**c**) Stator

(**d**) Permanent magnet

Figure 5. Temperature distribution under the rated condition.

3.2. Thermal Analysis of Two Modules and One Module under the Rated Condition

When there are different numbers of stator modules in the rated operation, the uneven distribution of copper loss in the circumferential direction will lead to circumferential heat transfer and to the asymmetric temperature distribution of stator in the circumferential direction. The maximum temperature of two modules or one module under the rated condition will be lower than the maximum temperature of all of the stator modules under the rated condition. Because the rotor is rotating, the temperature distribution of the rotor is symmetrically distributed in the circumferential direction; this paper mainly analyzes the temperature distribution of the stator parts.

Figure 6 shows the temperature distribution of the stator parts of two modules and one module under the rated condition. The maximum temperature of the end winding of two modules and one module under the rated condition decreased from 72.2 °C to 66.1 °C and 58.6 °C, respectively. The minimum temperature of the windings of the module under open-circuit conditions is 57.2 °C and 50.4 °C, respectively, and the temperature difference is 8.9 °C and 8.2 °C, respectively. The maximum temperature of the tooth of two modules and one module under the rated condition decreased from 67.8 °C to 59.7 °C and 53.1 °C, respectively. The minimum temperature of the tooth of the module under open-circuit conditions is 57.8 °C and 50.9 °C, respectively, and the temperature difference is 1.9 °C and 2.2 °C, respectively. The maximum temperature of the yoke of two modules and one module under the rated condition decreased from 64.2 °C to 58.2 °C and 51.5 °C, respectively. The minimum temperature of the yoke of the module under open-circuit

conditions is 54.5 °C and 48.4 °C, respectively, and the temperature difference is 3.7 °C and 3.1 °C, respectively. It can be seen from the results that the circumferential temperature difference of the winding is significantly higher than that of the tooth and yoke, because the insulation with low thermal conductivity in the slot exists in the heat transfer path in the circumferential direction and the circumferential heat transfer path is relatively long.
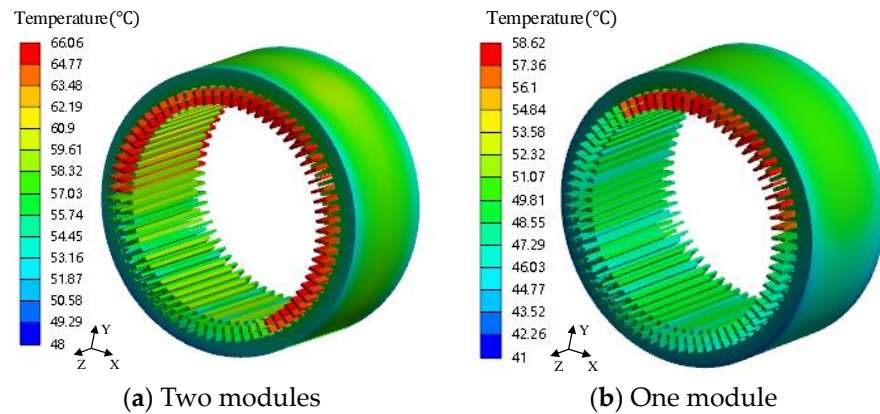

(**a**) Two modules																(**b**) One module

Figure 6. Winding temperature distributions under open-circuit conditions.

In the circumferential temperature distribution curve, the highest temperature in the axial direction is selected in Figure 7. For the open-circuit module and operating module, the highest temperature is at the middle position in the axial direction of the tooth and yoke. For the operating module, the highest temperature is at the end winding. For the open-circuit module, the highest temperature of the winding is at the middle position in the axial direction. This is because there is no copper loss in the winding of the open-circuit module, and there will be heat dissipation at the end winding and there will be circumferential heat conduction at the middle position in the axial direction. There is no copper loss in the open-circuit stator module, and the temperature of the tooth will be higher than that of the winding because of the existence of insulation. Because the yoke is closest to the housing, the temperature of the yoke is the lower than that of the tooth and winding.
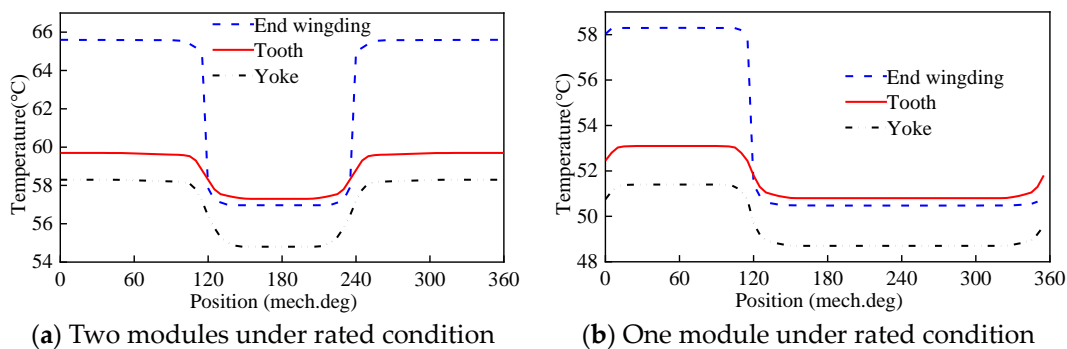

(**a**) Two modules under rated condition										(**b**) One module under rated condition

Figure 7. Winding temperature curve in the circumferential direction.

3.3. Thermal Analysis of Two Modules and One Module under the Fault-Tolerance Condition

When one or two stator modules are in the open-circuit condition, the rise in temperature of the other stator modules will decrease and output torque will decrease. The current healthy stator modules can be increased to increase the output torque. In order to keep the output torque unchanged, the current needs to be increased to 3 and 1.5 times the rated current when one module and two modules are in operation, respectively. The copper loss will be increased to 9 and 2.25 times the rated loss, respectively. Figure 8 shows the windings' temperature distribution of two modules and one module under the fault-tolerance condition. The maximum temperature rises to 105 °C when two modules

operate to produce the rated torque. The maximum temperature rises to 245.95 °C when one module operates to produce the rated torque. The insulation class is F and the maximum temperature allowable for insulation is 150 °C. When one module is in operation to produce the rated torque, the temperature of windings exceeded 150 °C, and the machine cannot operate at rated power for a long time. After iterative calculation, when the current of the healthy module is 2.3 times the rated current, the temperature is 150 °C. Moreover, the output torque is 0.76 times the rated torque.
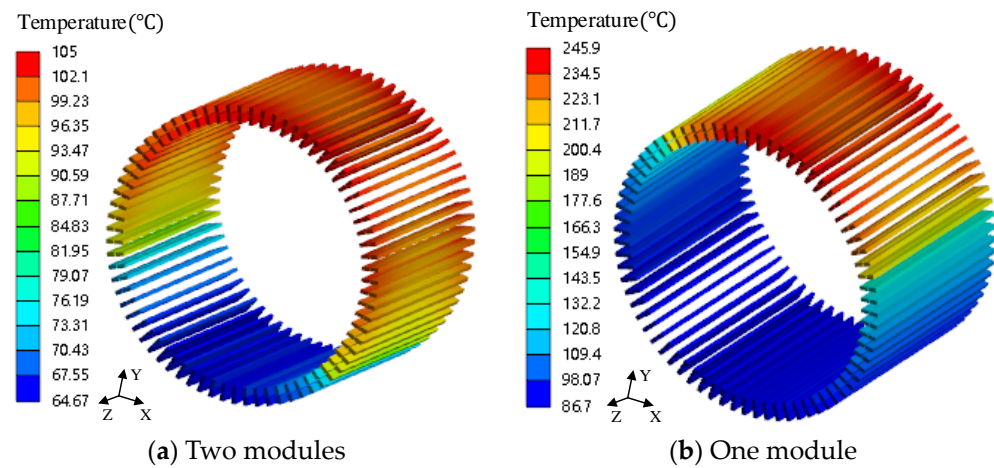

(a) Two modules   **(b)** One module

Figure 8. Winding temperature distributions under fault-tolerance conditions.

3.4. Thermal Analysis under One-Phase Open-Circuit Conditions

When the modular permanent magnet machine operates under one-phase open-circuit fault conditions, the output torque can be mainly unchanged by changing the amplitude and the two-phase current of the faulty module, keeping the current of the healthy modules unchanged. This is done in order to avoid the copper loss concentrated in the faulty module and to make the copper loss evenly distributed in the circumferential direction. The winding of the healthy modules can also be used for fault-tolerance control while the two-phase windings of the faulty module are used.

The sum of the magnetomotive force of all stator modules under fault-tolerance conditions is consistent with that under the rated condition. The phase current in the healthy module is a times that of the rated current, and the phase current in the faulty module is b times that of the rated current.

$$\sqrt{3}b + 6a = 9 \tag{5}$$

When only two-phase windings are used for fault tolerance, the fault-tolerant control strategy is named the constant magnetomotive force (MMF) strategy; the solution is $a = 1$ and $b = 1.732$.

In order to ensure the highest efficiency of the machine under fault-tolerance conditions, the minimum copper loss control strategy that ensures that the sum of copper loss of the faulty module and healthy module is at a minimum is proposed.

$$\min \left| 2b^2 + 6a^2 \right| \tag{6}$$

The solution is $a = 1.2$ and $b = 1.04$.

The same current fault-tolerance control strategy is that the amplitude of current of the faulty module and healthy module is same. The copper loss distribution under this control strategy is relatively even in the circumferential. The solution is $a = 1.164$ and $b = 1.164$.

In order to minimize the temperature of the machine, this paper proposes a zero-temperature-difference fault-tolerance control strategy. The zero-temperature-difference means that the maximum temperature of the faulty module and the health module are

the same. *a* and *b* need to be obtained by the iterative algorithm. The solution is $a = 1.159$ and $b = 1.181$. Figure 9 shows the calculation process of the zero-temperature-difference fault-tolerance strategy.
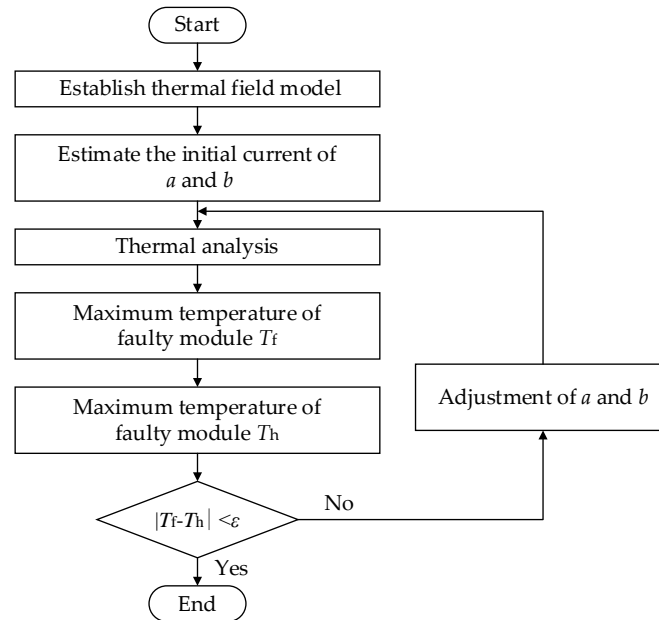

Figure 9. Flow chart of the zero-temperature-difference fault-tolerance strategy.

Figure 10 shows the copper loss distribution of each phase under different fault-tolerance control strategies. Figure 11 shows winding temperature curve in the circumferential direction under different fault-tolerance control strategies. Figure 12 shows the temperature distributions under the one-phase open-circuit condition with different fault-tolerance control strategies.
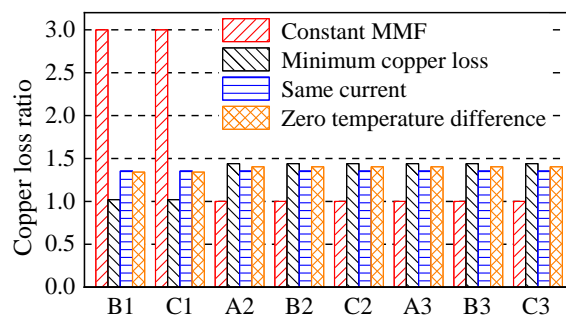

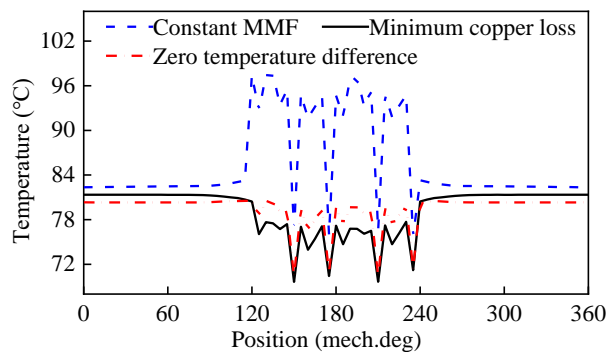**Figure 10.** Copper loss ratio of each phase under different fault-tolerance strategies.

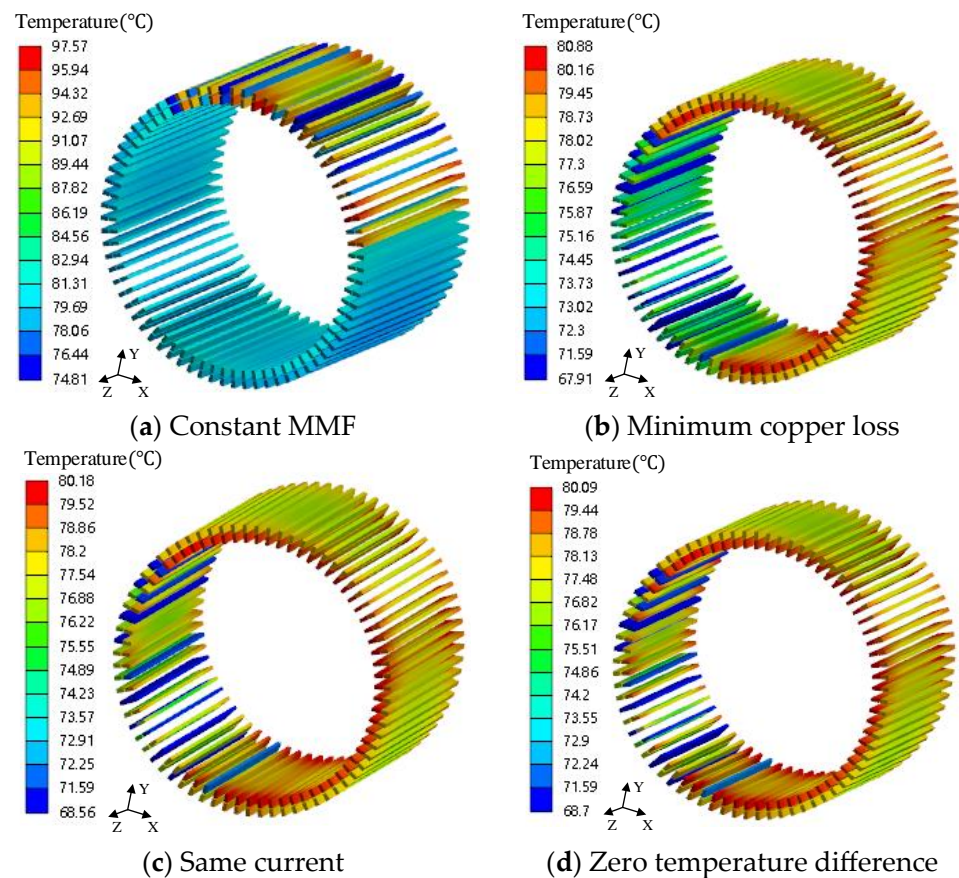**Figure 11.** Winding temperature curve in the circumferential direction.

Figure 12. Winding temperature distributions under the one-phase open-circuit condition.

The copper loss of the two-phase winding of the faulty module is three times that of the rated loss under the constant MMF control strategy. The copper loss is mainly concentrated in the faulty module, resulting in the winding temperature of the faulty module being much higher than that of the healthy module. The total copper loss of all windings under the minimum copper loss strategy is the smallest, because the current of the faulty stator module is relatively small and the winding temperature of the healthy module is higher than the temperature of the faulty module. The copper loss of all of the windings is the same under the same current control strategy, and the total copper loss of the faulty module is lower than that of each healthy module, so the temperature of the healthy module is slightly higher than that of the faulty module. The current ratio of different modules is adjusted to make the maximum temperature of faulty module the same as the maximum temperature of the healthy module under the zero-temperature-difference control strategy. It can be seen from the temperature curve in the circumferential direction that the temperature at the position where the upper and lower layers of the winding are open-circuit phase windings decreases most obviously, and the temperature at the position where one layer of the double-layer winding is an open-circuit phase winding also decreases to a certain extent.

Table 3 summarizes the current, copper loss, and maximum temperature of the modular combined permanent magnet machine under one phase open-circuit conditions with different fault-tolerance control strategies. The maximum temperature of the machine under the same current control strategy and the zero-temperature-difference control strategy are very close, because slot number of the stator module is large, resulting in the large thermal resistance in the circumferential heat transfer path. When the slot number of the module is small, the zero-temperature-difference fault-tolerance control strategy will significantly reduce the rise in temperature of the machine compared with other control

strategies. Therefore, this fault-tolerance control strategy is of great significance to improve the output torque under open-circuit fault-tolerance conditions.

Table 3. Comparison of different fault-tolerance strategies.

Control Strategy	a	b	Loss	Temperature (°C)
Rated	1	1	$9I^2R$	72.3
Constant MMF	1	1.732	$12I^2R$	97.6
Minimum copper loss	1.2	1.04	$10.8I^2R$	80.9
Same current	1.164	1.164	$10.84I^2R$	80.2
Zero temperature difference	1.159	1.181	$10.85I^2R$	80.1

4. Experimental Results

In order to verify the accuracy of the magneto–thermal coupling model established in this paper, a 30-pole 72-slot permanent magnet synchronous machine with three stator modules was designed and manufactured. The structure of the stator is shown in Figure 13. Each stator module has large-span and small-span coils. The test bench includes a torque-speed-measuring instrument, magnetic powder brake, and coupling. The inverter is manufactured by vacon and the switching frequency of the power electronic device used is 6 kHz. The power analyzer is manufactured by fluke. The temperature sensors used are PT100.
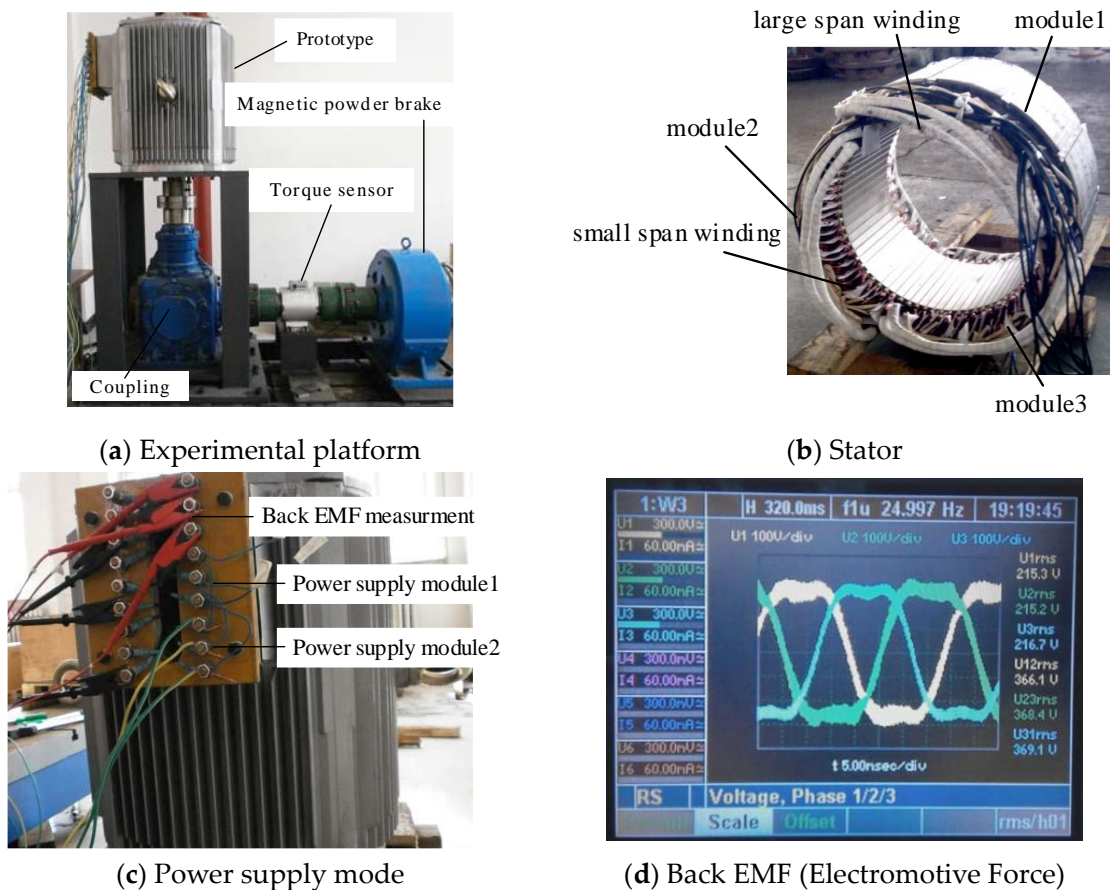

(**a**) Experimental platform

(**b**) Stator

(**c**) Power supply mode

(**d**) Back EMF (Electromotive Force)

Figure 13. Experimental test.

The experimental platform was built to test the rise in temperature of the prototype. The experimental platform is shown in Figure 13. The prototype is powered by a conventional inverter, and the three-phase windings of each stator module are equivalent to the other modules. The operation of different numbers of stator modules is achieved by the

corresponding parameter settings of the inverter according to the parallel relationship. The experiment of one-phase open-circuit conditions with different fault-tolerance control strategies was not carried out. Figure 13 shows the measurement method and power supply mode of the modular permanent magnet machine.

The predicted and experimental results of different numbers of modules in operation are shown in Table 4; the predicted results are in good agreement with the experimental results, and the experimental results are higher than the predicted results. Because the thermal model ignores the end of the large-span coil and the end of the large-span coil is too long, the temperature of the end of large-span coil will be higher than the end of the small-span coil, and heat will be transferred to the middle position of the module in the circumferential direction.

Table 4. Comparison of the calculated and experimental results.

Operating Conditions	Calculated (°C)	Measured (°C)
One module under rated condition	58.6	63.8
Two modules under rated condition	66.1	72.6
Three modules under rated condition	72.2	79.6
One module rated under fault-tolerance condition	150	165.2
Two modules rated under fault-tolerance condition	105	114.6

The windings of one stator module are independent of the windings of the other modules, and the mutual inductance between the modules is very small. The power supply mode of two modules in operation is shown in Figure 13, and the third module is in the open-circuit condition. The no-load back EMF of the module can be directly measured. By comparing the no-load back EMF in all conditions to the no-load back EMF in the cold state, the temperature of the permanent magnet can be estimated in real time according to the remanence temperature coefficient of the permanent magnet. The main consideration of this paper is to study the asymmetry temperature distribution of stator and windings in the circumferential direction. The temperature distribution of permanent magnets in the circumferential direction is symmetrical because they are rotating. The rotational speed of the prototype is low and the temperature of the permanent magnet is lower than the temperature of the end windings. The temperature of the permanent magnets was not analyzed in detail in this paper. For high-speed modular permanent magnet machines, the temperature of the permanent magnet will be higher than that of the end winding, and it is necessary to study the temperature of permanent magnets. It provides a simple and effective method for the real-time monitoring of the temperature of permanent magnets.

5. Discussion

The aim of this research was to investigate the temperature distributions of the modular permanent magnet machine under open-circuit conditions and to predict the output torque under open-circuit conditions considering the temperature limit of insulation. The consideration of the investigation was around the temperature distribution in the circumferential direction. The temperature of the machine under the rated condition was calculated. Temperature distributions of different numbers of stator modules in operation were analyzed. For the one-phase open-circuit fault condition, the temperature distributions of stators with different fault-tolerance control strategies were compared. The temperature of the machine under the one-phase open-circuit condition with the zero-temperature-difference control strategy will be 0.8 °C lower than that with the minimum copper loss control strategy. If the temperature of the machine cannot be accurately predicted under fault conditions, it will cause the temperature of windings t be higher than the limit of insulation or insufficient output torque.

A prototype with three stator modules was manufactured, and the results were verified by experimental test. It is of great significance for the accurate calculation of a machine with asymmetric temperature distribution in the circumferential direction.

6. Conclusions

A modular permanent magnet machine is composed of several stator modules and the windings of each module can be controlled independently. The modular permanent magnet machine has excellent abilities in terms of fault tolerance. The temperature distributions of the modular permanent magnet machine under open-circuit conditions with uneven copper loss distribution were analyzed. Owing to the uneven copper loss distribution in the circumferential direction, heat transfer occurs in the circumferential direction and temperature distributions are asymmetric in the circumferential direction. The temperature will rise sharply if only the other two-phase windings of the faulty module are used to compensate the torque under the single-phase open-circuit condition. The temperature can be reduced by using the two-phase windings of the faulty module and the windings of the healthy modules together for fault tolerance. The principle of the fault-tolerance strategy is to make the loss evenly distributed in the circumferential direction and to make the maximum temperatures of healthy and faulty modules uniform.

Author Contributions: Y.L. wrote the paper; B.Z. supervised all processes; M.Z. analyzed the data; G.F. checked the paper format. All authors have read and agreed to the published version of the manuscript.

Data Availability Statement: Not applicable.

References

1. Jiang, X.; Huang, W.; Cao, R.; Hao, Z.; Jiang, W. Electric Drive System of Dual-Winding Fault-Tolerant Permanent-Magnet Motor for Aerospace Applications. *IEEE Trans. Ind. Electron.* **2015**, *62*, 7322–7330. [CrossRef]
2. Wang, Y.; Hao, W. General Topology Derivation Methods and Control Strategies of Field Winding-Based Flux Adjustable PM Machines for Generator System in More Electric Aircraft. *IEEE Trans. Transport. Electrific.* **2020**, *6*, 1478–1496. [CrossRef]
3. Wu, L.; Zhu, J.; Fang, Y. A Novel Doubly-Fed Flux-Switching Permanent Magnet Machine with Armature Windings Wound on Both Stator Poles and Rotor Teeth. *IEEE Trans. Ind. Electron.* **2020**, *67*, 10223–10232. [CrossRef]
4. Sui, Y.; Yin, Z.; Cheng, L.; Zheng, P.; Tang, D. Multiphase Modular Fault-Tolerant Permanent-Magnet Machine with Hybrid Single/Double-Layer Fractional-Slot Concentrated Winding. *IEEE Trans. Magn.* **2019**, *55*, 7500506. [CrossRef]
5. Zhou, H.; Xu, J.; Chen, C.; Tian, X.; Liu, G. Disturbance-Observer-Based Direct Torque Control of Five-Phase Permanent Magnet Motor Under Open-Circuit and Short-Circuit Faults. *IEEE Trans. Ind. Electron.* **2021**, *68*, 11907–11917. [CrossRef]
6. Guo, H.; Guo, S.; Xu, J.; Tian, X. Power Switch Open-Circuit Fault Diagnosis of Six-Phase Fault Tolerant Permanent Magnet Synchronous Motor System under Normal and Fault-Tolerant Operation Conditions Using the Average Current Park's Vector Approach. *IEEE Trans. Power Electron.* **2021**, *36*, 2641–2660. [CrossRef]
7. Tang, H.; Li, W.; Li, J.; Gao, H.; Wu, Z.; Shen, X. Calculation and Analysis of the Electromagnetic Field and Temperature Field of the PMSM Based on Fault-Tolerant Control of Four-Leg Inverters. *IEEE Trans. Energy Convers.* **2020**, *35*, 2141–2151. [CrossRef]
8. Wang, W.; Zhang, J.; Cheng, M. Common Model Predictive Control for Permanent-Magnet Synchronous Machine Drives Considering Single-Phase Open-Circuit Fault. *IEEE Trans. Power Electron.* **2017**, *32*, 5862–5872. [CrossRef]
9. Zhang, B.; Gan, B.; Li, Q. Analysis of a Fault-Tolerant Module-Combined Stator Permanent Magnet Synchronous Machine. *IEEE Access* **2020**, *8*, 70438–70452. [CrossRef]
10. Gan, B.; Zhang, B.; Li, Q.; Feng, G.; Li, G. Research on Operation of Low-Speed and High-Torque Module Combined Stator Permanent Magnetic Fault-Tolerant Motor with Unequal Span Winding. *IEEE Access* **2020**, *8*, 166824–166838. [CrossRef]
11. Mo, L.; Zhang, T.; Lu, Q. Thermal Analysis of a Flux-Switching Permanent-Magnet Double-Rotor Machine With a 3-D Thermal Network Model. *IEEE Trans. Appl. Supercond.* **2019**, *29*, 0600905. [CrossRef]
12. Zhao, W.; Cao, D.; Ji, J.; Huang, L.; Liu, T. A Generalized Mesh-Based Thermal Network Model for SPM Machines Combining Coupled Winding Solution. *IEEE Trans. Ind. Electron.* **2021**, *68*, 116–127. [CrossRef]
13. Tong, W.; Sun, R.; Li, S.; Tang, R. Loss and Thermal Analysis for High-Speed Amorphous Metal PMSMs Using 3-D Electromagnetic-thermal Bi-Directional Coupling. *IEEE Trans. Energy Convers.* **2021**, *36*, 2839–2849. [CrossRef]
14. Qi, J.; Hua, W.; Zhang, H. Thermal Analysis of Modular-Spoke-Type Permanent-Magnet Machines Based on Thermal Network and FEA Method. *IEEE Trans. Magn.* **2019**, *55*, 8104105. [CrossRef]
15. Taras, P.; Li, G.; Zhu, Z.; Foster, M.; Stone, D. Combined Multiphysics Model of Switched Flux PM Machines under Fault Operations. *IEEE Trans. Ind. Electron.* **2019**, *66*, 6737–6745. [CrossRef]

16. Tang, H.; Di, J.; Wu, Z.; Li, W. Temperature Analysis for the Asymmetric Six-Phase Permanent Magnet Synchronous Motor in Healthy and Fault-Tolerant Modes. *IEEE Trans. Ind. Electron.* **2023**, *70*, 6482–6493. [CrossRef]
17. Shi, Y.; Wang, J.; Wang, B. Transient 3-D Lumped Parameter and 3-D FE Thermal Models of a PMASynRM under Fault Conditions with Asymmetric Temperature Distribution. *IEEE Trans. Ind. Electron.* **2021**, *68*, 4623–4633. [CrossRef]